







Eco-Friendly Synthesis of Bioactive Silver Nanoparticles Using *Astragalus fasciculifolius* Extracts: Regional Phytochemical Variation and Biomedical Potential

Fatemeh Nosrati¹ , Barat Ali Fakheri¹ , Habib Ghaznavi² , Nafiseh Mahdinezhad¹ , Roghayyeh Shirvalilu² , Bahman Fazeli-Nasab^{3✉} 

¹Department of Plant Breeding and biotechnology, Faculty of Agriculture, University of Zabol, 9861335856 Zabol, Iran

²Pharmacology Research Center, Zahedan University of Medical Sciences, 9816743463 Zahedan, Iran

²Department of Agronomy and Plant Breeding, Agriculture Institute, Research Institute of Zabol, Zabol, Iran

Article Info	ABSTRACT
Article type: Original Article	Objective: Green synthesis of nanoparticles has emerged as a promising strategy in material science and nanotechnology. In this study, silver nanoparticles (AgNPs) were synthesized through a cost-effective, environmentally friendly, and highly efficient process. Bioreduction was carried out at room temperature using aqueous root and gum extracts of <i>Anzaroot</i> (<i>Astragalus fasciculifolius</i> Bioss).
Article History: Received: 26 Jun 2025 Revised: 11 Jul 2025 Accepted: 13 Jul 2025 Published Online:	Methods: Roots and gum of <i>A. fasciculifolius</i> were collected from six locations in Sistan-Baluchestan Province (Table 1). Aqueous extracts (10 g/100 mL) were prepared and analyzed for total phenolics (Folin-Ciocalteu), flavonoids (AlCl ₃), and carbohydrates (phenol-sulfuric acid). AgNPs were biosynthesized using 1, 3, and 5 mM AgNO ₃ solutions, with 1 mM identified as optimal. Nanoparticles were characterized by UV-Vis spectroscopy, TEM, and XRD. Antioxidant activity (DPPH assay) and antimicrobial activity (MIC/MBC) were assessed against four bacterial strains. GC-MS (Agilent 7890A) was performed using an HP-5 MS column.
✉ Correspondence to: Bahman Fazeli-Nasab	Results: GC-MS analysis revealed pronounced regional differences in gum composition: Khash samples were rich in aliphatic hydrocarbons, Sarava samples contained pharmaceutical-like compounds (pilocarpine, gabapentin derivatives), and Sarbaz gum showed unique nitrogenous constituents (17.52% urea derivatives), suggesting environmental adaptation. ANOVA indicated significant location-dependent differences ($p < 0.01$) in phenolic content (mean 32.41 mg GAE/g), with Poshtkuh showing the highest accumulation (42.61 mg GAE/g). Flavonoids ranged from 0–2.0 mg QE/g, while carbohydrate levels (mean 366.93 mg GE/g) displayed habitat-specific variation ($p < 0.01$). Biosynthesized AgNPs exhibited surface plasmon resonance at 400–500 nm and crystalline peaks at 38°, 43°, 64°, and 77.3° (XRD). TEM confirmed spherical AgNPs (5–50 nm), with gum-derived nanoparticles (23.29 nm) demonstrating superior DPPH scavenging (98.40% at 500 µg/mL) compared with root-derived AgNPs (81.41%). Antimicrobial assays (400 µg/mL) showed enhanced Gram-negative inhibition (MIC 3.12–50 µg/mL), whereas crude extracts were more active against Gram-positive strains.
Email: bfazelinasab@gmail.com	Conclusion: This study highlights the diverse phytochemistry, regional variability, and bioactivity of <i>A. fasciculifolius</i> gum, underscoring its potential applications in antimicrobial, antioxidant, and nanomedicine research. The biosynthesized AgNPs demonstrated potent antioxidant and Gram-selective antibacterial properties. Further studies should investigate environmental drivers of metabolite production, elucidate pharmacological mechanisms, and develop scalable AgNP synthesis for therapeutic use.
	Keywords: Anzaroot (<i>Astragalus fasciculifolius</i> Bioss), <i>Bacillus cereus</i> , <i>Escherichia coli</i> , <i>Pseudomonas aeruginosa</i> , <i>Staphylococcus aureus</i>
➤ How to cite this paper	
Nosrati F, Ali Fakheri B, Ghaznavi H, Mahdinezhad N, Shirvalilu R, Fazeli-Nasab B. Eco-Friendly Synthesis of Bioactive Silver Nanoparticles Using <i>Astragalus fasciculifolius</i> Extracts: Regional Phytochemical Variation and Biomedical Potential. <i>Plant Biotechnology Persa</i> . 2026 8(1); Proof.	

Introduction

Each day, new evidence highlights the harmful effects of chemical preservatives on human health, including their carcinogenic and teratogenic properties, as well as the toxic residues they leave behind. Consequently, there is an increasing demand for food products that can naturally extend their shelf life. In response, food researchers are investigating alternatives to these harmful preservatives, with one promising option being hydrolyzed proteins derived from plants and animals. These hydrolyzed proteins consist of bioactive peptides, which are low molecular weight compounds known for their natural antioxidant properties [1-4].

The increasing occurrence of bacterial infections has sparked interest among researchers in developing various antibacterial agents. Nevertheless, the observation of antibiotic resistance among bacterial strains during recent years has raised concerns about how to tackle these pathogens in the future. Official reports indicate a surge in the rate of infection and deaths caused by super-resistant bacterial strains over the past decade. Not only, do bacteria develop antibiotic resistance through various mechanisms, but also they rapidly evolve and improve their resistance mechanisms if only a small colony survives in the presence of antibiotics. The widespread and excessive use of antibiotics has also contributed to the emergence and spread of antibiotic resistance among different strains. Given this knowledge, it is crucial to develop new methods and explore new substances with antibacterial properties in order to combat the increasing resistance of pathogenic agents [2, 5, 6].

Metal and metal oxide nanoparticles are promising candidates due to their high surface-to-volume ratio, which translates into heightened activity against microbes. Moreover, metal nanoparticles offer exceptional properties and great potential in biomedical applications, without any harmful effects of large quantities of metals and their ions on human health [2, 5, 6]. Consequently, scientists have been searching for safer methods to produce nanomaterials, such as green synthesis using fungi [7], bacteria, or plants [8].

The medicinal plant *A. fasciculifolius* Bioss (Anzaroot), a member of the Fabaceae family, is

renowned for its bioactive compounds, including glycosides, saponins, phenolics, and polysaccharides. It exhibits anticancer, anti-inflammatory, antiviral, and antibacterial properties [9,11-13]. Iran is the primary global supplier of gum tragacanth from *Astragalus* species, traditionally used for gastrointestinal, hepatic, and metabolic disorders. Phytochemical studies confirm the presence of saponins, alkaloids, and phenolic compounds, making it a valuable candidate for natural therapeutics [14, 15].

The eco-friendly biosynthesis of silver nanoparticles (AgNPs) using plant extracts has gained attention due to its sustainability and efficiency. *A. fasciculifolius* extracts, rich in polysaccharides and phenolics, serve as effective reducing and stabilizing agents for AgNPs. These biogenic nanoparticles exhibit superior antimicrobial and antioxidant properties compared to chemically synthesized counterparts, offering potential against multidrug-resistant pathogens like *Pseudomonas aeruginosa* and *Staphylococcus aureus* [16-19]. This study aimed to investigate the phytochemical composition and bioactive potential of *A. fasciculifolius* Bioss, focusing on its root and gum extracts. The research evaluated total flavonoids, phenolics, and carbohydrate content, synthesized silver nanoparticles (AgNPs) using plant extracts, and assessed their antioxidant and antibacterial properties. Additionally, gas chromatography-mass spectrometry (GC-MS) was employed to characterize bioactive compounds, providing insights into the plant's medicinal applications.

Materials and methods

Area Selection and Sample Collection

To determine the distribution range of the target plant species, potential habitats were initially identified using primary sources, including Trees and Shrubs of Iran (Mozaffarian, 2004), consultations with experts from the Natural Resources Departments of various counties, and field surveys. Following habitat identification, three counties were selected, with two sampling areas per county: Saravan (Saravan, Nahoak), Mehrestan (Birak, Mehrestan), and Khash (Poshtkuh, Panjanganst) (Table 1).

Table 1: Geographical coordinates of *A. fasciculifolius* collection sites

No.	County	Locality	Longitude (E)	Latitude (N)	Elevation (m asl)
1	Saravan	Saravan	62°17'11.19"	27°17'30.8"	1,196
2		Nahoak	62°21'11.5"	27°33'50.3"	1,394
3	Mehrestan	Birak	61°40'56.8"	27°13'15.4"	1,345
4		Anjirak	61°17'51.7"	27°19'14.7"	1,413
5	Khash	Poshtkuh	61°93'42.5"	28°98'25.8"	1,416
6		Panjangasht	61°97'41.8"	28°61'18.9"	1,557

Plant Material

The roots and gums of *A. fasciculifolius* Bioss were collected on June 2022. The voucher specimen was confirmed by the Department of Botany, University of Tehran, Iran, with the herbarium code of PMP-874 (figure 1). Fresh roots and gum of *A. fasciculifolius* were carefully washed and allowed to air-dry. The specimens were then ground into a fine powder using an electric grinder. To prepare each plant Aqueous extract, 10 g of the powdered root and

gum was thoroughly mixed with 100 mL of water and left at room temperature for 24 hours. The heterogeneous mixture was subjected to precision filtration utilizing Whatman No. 1 cellulose filter media. The clarified filtrate was preserved as a primary stock solution at 4°C and immediately employed in the eco-friendly biosynthesis of silver nanoparticles (AgNPs). Concurrently, an aliquot of the extract was concentrated via vacuum-assisted solvent evaporation and archived at 4°C for subsequent analytical characterization.



Figure 1: *A. fasciculifolius* Bioss, plant, a: Shrub b: A sample of leaves and flowers, c: Gum, d: Root

Synthesis of AgNPs Silver nitrate (AgNO₃)

Solutions containing 1 and 5 mM of silver nitrate were made. After that, 200 mL of plant Aqueous extract and 100 mL of solution containing 1 and 5 mM of silver nitrate were added respectively. Then,

the total volume reached 500 mL after double distillation. The color of the solution changed from colorless to brown, which shows that the silver ions (Ag⁺) have been reduced to silver nanoparticles (Ag⁰). The absorbance of the solution was evaluated using a UV-Vis spectrophotometer (Jenway 6715) after a short period of time.

Characterization of AgNPs

Optical absorption spectra of the biosynthesized nanoparticles were acquired using a dual-beam UV-Vis-NIR spectrophotometer to evaluate their photonic properties across different synthesis parameters. Spectral scanning was performed under ambient conditions ($25 \pm 1^\circ\text{C}$) spanning 350–800 nm, demonstrating a characteristic surface plasmon resonance (SPR) band in the visible spectrum. Complementary structural characterization was performed through high-resolution transmission electron microscopy (HR-TEM, Philips CM-30, 120 kV accelerating voltage, 2.5 Å resolution) and polycrystalline X-ray diffraction analysis. For TEM specimen preparation, purified nanoparticle suspensions were ultrasonically dispersed in ethanol, deposited onto 300-mesh carbon-coated copper grids, and dried under IR irradiation. Crystallite dimensions were calculated from PXRD patterns using the Debye-Scherrer approximation of peak broadening at full-width half-maximum (FWHM).

Gas Chromatography (GC) Specifications of GUM extract

The analytical procedure was executed utilizing an Agilent 7890B gas chromatographic (GC) system, incorporating a split/splitless injection port coupled with a 5977A mass spectrometric (MS) detector. The mass spectrometer was configured in electron impact (EI) ionization mode with an electron energy of 70 eV. Ultra-high-purity helium (99.99%) was employed as the mobile phase at a constant flow rate of 1 mL/min. Chromatographic separation was achieved using a capillary column (30 m \times 0.25 mm) coated with an HP-5 MS stationary phase. The oven temperature was initiated at 60 °C and held isothermally for 2 min, followed by a linear gradient of 6 °C/min until attaining a final temperature of 250 °C, which was sustained for 4 min. The operational temperatures for the transfer line, ionization chamber, mass filter, and injection port were maintained at 280 °C, 230 °C, 150 °C, and 280 °C, respectively.

Determination of Total Flavonoid Content

The quantification of total flavonoids was performed via an aluminum chloride-based chromogenic assay [20]. Specifically, 1 mL of the gum-derived aqueous extract was combined with 1.5 mL of methanol, 0.1

mL of 10% aluminum chloride (in methanol), 0.1 mL of 1 M potassium acetate, and 2.8 mL of deionized water. Following a 30-minute incubation period under ambient conditions, the absorbance was recorded at 415 nm using a BTS-45 spectrophotometer (Model: BTS-0638). Quercetin (Sigma Chemical Co.) served as the reference standard, with a calibration curve established across a concentration range of 250–1000 µg/mL in methanol. The flavonoid content was subsequently calculated and reported as milligrams of quercetin equivalents per gram of sample (mg QE/g). Each measurement was conducted in triplicate to ensure reproducibility.

Determination of Total Phenolic Content

The determination of total polyphenolic compounds was conducted employing the Folin-Ciocalteu spectrophotometric method [21]. The analytical procedure involved the addition of 5 mL Folin-Ciocalteu oxidant to 1 mL of either the gum matrix aqueous extract or gallic acid calibration standard, subsequently mixed with 4 mL of sodium carbonate solution (1 M). Following a 15-minute reaction period under ambient temperature conditions, spectral absorbance measurements were obtained at 765 nm wavelength utilizing a BTS-45 benchtop spectrophotometer (Model BTS-0638). Quantitative analysis derived from the standard curve enabled expression of results in milligram gallic acid equivalents per gram of dry mass (mg GAE/g). Analytical replicates (n=3) were performed for each sample to ensure methodological precision.

Determination of Carbohydrate Content (Total Soluble Sugars)

The quantification of water-soluble carbohydrates was performed employing the phenol-sulfuric acid spectrophotometric assay [22, 23]. Precisely 0.2 g of the gum specimen was homogenized with 10 mL deionized water in hermetically sealed glass tubes, followed by thermal treatment at 100°C for 15 minutes in a precision-controlled water bath. Following thermal equilibration to ambient temperature, 1 mL aliquot of the hydrolysate was reacted with 1 mL of 5% (w/v) aqueous phenol solution and 5 mL concentrated sulfuric acid (98% v/v). Spectrophotometric analysis was conducted at $\lambda=488$ nm using a BTS-45 UV-Vis spectrophotometer (Model BTS-0638). The total

sugar content was derived from a glucose standard curve and expressed as milligram glucose equivalents per gram of dry matter (mg GE/g). All analytical procedures were executed in triplicate to ensure methodological reproducibility.

DPPH Free Radical Scavenging Assay

The free radical scavenging capacity of both crude Aqueous extracts (root and gum) from *A. fasciculifolius* Bioss and their corresponding biogenic silver nanoparticles was evaluated through 2,2-diphenyl-1-picrylhydrazyl (DPPH) radical inhibition assay [1]. Serial dilutions (100-500 µg/mL in 100 µg increments) of each test specimen were prepared. Aliquots (2 mL) of these solutions were reacted with an equal volume of 0.1 mM methanolic DPPH solution under light-protected conditions (25±1°C, 30 min incubation). Spectrophotometric quantification was performed at λ=517 nm using a Shimadzu UV-1800 spectrophotometer, with radical inhibition percentages calculated relative to blank controls according to the standard equation:

$$\% \text{ Inhibition} = \left[\frac{A_{\text{Control}} - A_{\text{Sample}}}{A_{\text{Control}}} \right] * 100$$

Antibacterial Assays

The antimicrobial efficacy of *A. fasciculifolius* phytoconstituents (root/gum Aqueous extracts) and their corresponding biosynthesized silver nanoparticles was evaluated against four clinically relevant bacterial pathogens: *Bacillus cereus* (PTCC 1665), *Staphylococcus aureus* (PTCC 1189), *Pseudomonas aeruginosa* (PTCC 1310), and *Escherichia coli* (PTCC 1399), procured from the microbial repository of Zahedan University of Medical Sciences. Standardized microbial suspensions (0.5 McFarland turbidity standard) were prepared spectrophotometrically and subjected to 1:300 dilution. Stock solutions of nanoparticles (400 µg/mL in sterile aqueous matrix) were systematically diluted in 96-well microtiter plates. The microdilution assay was initiated by aliquoting 20 µL of nanoparticle suspension into duplicate primary wells, followed by serial two-fold dilutions across subsequent wells. Each well received 80 µL of Mueller-Hinton broth and 100 µL of standardized inoculum, creating final nanoparticle concentrations ranging from 400 to 3.125 µg/mL. Plates were incubated under agitation (37°C, 24 h) in a

controlled-environment orbital shaker. The minimum inhibitory concentration (MIC) was determined as the lowest nanoparticle concentration exhibiting complete optical clarity. For minimum bactericidal concentration (MBC) determination, aliquots from clear wells were streaked onto Mueller-Hinton agar and incubated (37°C, 24 h). All assays were performed in triplicate with complete methodological reproducibility (zero standard deviation across replicates).

Efficacy of the Extraction Method

In order to obtain the right Aqueous extract and check the effective substance, it is necessary to consider several factors including the plant material, the choice of the right solvent, and accuracy in the steps and method of extraction. The Soxhlet method is a standard extraction method that has been widely used due to its advantages such as easy use, continuous contact of extractive materials with fresh solvent, use of high temperature for complete and fast extraction, and no need for filtration [24]. The choice of solvent is very important in all extraction methods, so that the choice of different solvents will create different extracts with different compositions [25]. The extraction process was carried out using 10 grams of dried ketira in a Soxhlet apparatus for 8 hours. Ethanol was used as the solvent. Following ethanol evaporation, the desired extract was stored in a refrigerator at 4 degrees Celsius for future analysis [26].

Statistical analysis

In this research it was used Solvent blank as a control negative and ampicillin as a control positive. Data were analyzed using Statistix ver 10, ANOVA followed by Tukey's post hoc test. Significance set at $p < 0.05$. Results are reported as mean ± SD.

Results

Ingredients of *A. fasciculifolius* gum extract

The gum from Khash (1) exhibits a diverse chemical profile, with 1,3-dimethylbenzene (2.59%) and 1,3-cyclopentadiene derivatives (5.38%) as key volatiles. Notably, nonane (3.92%) and eicosane (3.90%) suggest a prevalence of aliphatic hydrocarbons, while diaziridine derivatives (2.90%) hint at nitrogen-containing compounds. The

presence of tetrachloromethane (2.66%) raises questions about environmental interactions, though its origin warrants further study. In Khash (2), nonane (6.42%) and octane (6.80%) dominate, reflecting a stronger alkane signature than Khash (1). The sample also contains unique heterocycles like isothiazole (2.04%) and oxirane derivatives (4.53%), which may contribute to bioactivity. The high dodecane concentration (9.43%) distinguishes this region, alongside unexpected pharmaceuticals like tilidine (6.03%), suggesting potential exogenous contamination or metabolic synthesis. Sarava (1) stands out with pilocarpine (9.51%) and paracetamol (4.03%), both atypical for plant gums. The dominance of oleic acid (26.08%) and linoleic acid (2.28%) indicates a lipid-rich matrix, while nonadecane (5.35%) aligns with regional alkane patterns. The absence of minor compounds in this sample contrasts sharply with other sites, implying distinct ecological or extraction influences. Sarava (Nahoak) (2) features camphor (2.21%) and gabapentin derivatives (6.53%), alongside naphthalene analogs (8.30%). The high terbutaline content (5.88%) is unusual and may reflect soil contaminants. Oxalic acid esters (5.01%) suggest adaptations to oxidative stress, while the reappearance of tilidine (5.46%) across Khash and Sarava hints at cross-regional environmental factors. Mehrestan's gum is marked by ethanamine derivatives (2.75%) and 5-methyl-1-hexene (5.72%), indicating nitrogen assimilation and branched alkane synthesis. Pilocarpine reappears (1.95%), but at lower levels, while dodecane (7.35%) and ibuprofen metabolites (1.92%) suggest hybrid biochemical pathways. The sample's high ethirimol (5.84%) content implies fungal interactions. Sarbaz's profile is exceptional, with a urea derivative (17.52%) as the dominant compound, rarely reported in plant gums. Azetidine (2.87%) and chloroform (4.38%) indicate unique halogenation processes. The presence of mefruside (2.23%) and DOM (4.55%)—a stimulant—raises intriguing questions about soil chemistry or anthropogenic exposure in this region (Table 2).

The GC-MS results reveal striking regional variations in the chemical composition of *A. fasciculifolius* gum, highlighting the influence of environmental and ecological factors. Khash samples (1 & 2) are dominated by aliphatic hydrocarbons like nonane and octane, but Khash (2) uniquely contains higher levels of dodecane (9.43%) and pharmaceutical-like compounds such as tilidine

(6.03%). In contrast, Sarava (Nahoak) samples exhibit unusual medicinal constituents—pilocarpine (9.51%) in Sarava (1) and gabapentin derivatives (6.53%) in Sarava (2)—alongside high terpene and lipid content, suggesting possible microbial or soil interactions. Mehrestan's gum is distinguished by nitrogen-rich compounds (e.g., ethanamine derivatives) and branched alkanes, while Sarbaz stands out with an exceptionally high urea derivative (17.52%) and halogenated compounds like chloroform (4.38%), implying unique metabolic or environmental stress responses. Overall, the data underscore how geography shapes phytochemistry, with Khash favoring alkanes, Sarava accumulating drug-like molecules, and Sarbaz producing rare nitrogenous compounds, each suggesting distinct adaptive strategies.

Total Phenolic Content

Statistical evaluation via one-way analysis of variance (ANOVA) indicated highly significant disparities ($p < 0.01$) in the concentration of phenolic compounds across distinct ecological zones (location \times county interaction), with county-specific variations demonstrating significance at $p < 0.05$ (refer to Table 3). Subsequent Duncan's multiple range test corroborated statistically meaningful differentiation ($p < 0.05$) among sampled populations. The mean phenolic content, expressed as gallic acid equivalents per gram of dry mass (mg GAE/g), was quantified at 32.41 (Table 4). Maximum phenolic accumulation (42.61 mg GAE/g) was detected in specimens from the Poshtkuh region, whereas minimal levels (28.1 mg GAE/g) were documented in the Nahoak population.

Total Flavonoid Content

ANOVA indicated statistically significant variations ($p < 0.01$) in total flavonoid content among *A. fasciculifolius* populations (Table 3). The mean flavonoid content across all samples was 1.48 mg quercetin equivalent per gram (mg QE/g). The Nahoak population exhibited the highest flavonoid concentration (2.0 mg QE/g), while the lowest level (0 mg QE/g) was detected in Birak (Table 4).

Table 2: Ingredients of A. fasciculifolius gum extract

Khash (1)		Khash (2)		Sarava (Nahoak)(1)		Sarava (Nahoak)(2)		Mehrestan		Sarbaz	
Compositions	%	Compositions	%	Compositions	%	Compositions	%	Compositions	%	Compositions	%
Benzene, 1,3-dimethyl-	2.59	Benzene, 1,3-dimethyl-	4.01	Nonadecane	5.35	Benzene, 1,3-dimethyl-	5.06	Benzene, 1,3-dimethyl-	3.23	2-Amino-oxazole	2.14
1,3-Cyclopentadiene, 5-(1-methyl...	5.38	Nonane	6.42	Naphthalene, decahydro-1,6-dimet	9.32	Nonane	4.80	Nonane	5.04	Oxirane, hexyl	2.55
Nonane	3.92	Octane	6.80	Pilocarpine	9.51	Octane	4.87	Hexane, 2,3,3-trimethyl-	2.74	Benzene, 1,3-dimethyl	4.77
Eicosane	3.90	Hexane, 2,3,3-trimethyl-	3.93	Paracetamol	4.03	Oxalic acid, cyclohexyl isobutyl...	5.01	Oxirane, (2-methylpropyl)-(CAS)...	2.90	Octane, 2,4,6-trimethyl	2.75
Nonadecane	3.92	Oxirane, (2-methylpropyl)-(CAS)...	4.53	1-Octadecyne	4.17	Tilidine-M	5.46	Octane	3.03	Azetidine, 1,2-dimethyl	2.87
Hexane, 2,3,3-trimethyl-	2.76	Eicosane	4.05	MECC	4.58	Nonadecane	3.45	Ethanamine, N-methyl-	2.75	Undecane	2.75
Tetrachloromethane	2.66	Isothiazole	2.04	Ethinamate	4.39	Camphor	2.21	1H-Tetrazol-5-amine	1.34	1-Pentanol, 2,2-dimethyl-	1.89

2-Propanone, hydrazone	2.91	1H-Tetrazol-5-amine	2.17	Apiol	26.08	Naphthalene, decahydro-2-methyl	2.28	Eicosane	1.80	Mefruside	2.23
Diaziridine,3,3-dimethyl-	2.90	Ethanamine, N-methyl-	2.30	Pirprofen-M	26.47	trans,cis-1,8-Dimethylspiro	6.25	5-Methyl-1-hexene	5.72	Diaziridine,3,3-dimethyl-	2.01
Octane	2.92	Tilidine-M	6.03	Oleic Acid	1.92	Gabapentin -H2O ME	6.53	Tilidine-M	6.13	1,4,7,10,13,16-Hexaoxacycloeicos	2.24
Isothiazole	1.45	5-Methyl-1-hexene	6.16	Linoleic acid	2.28	Paracetamol	6.82	2-Methyl-1-pentene	6.16	Tetrahydrofuran	2.35
1H-Tetrazol-5-amine	1.52	Oxalic acid, allyl nonyl ester	3.92	Nomifensine AC	1.92	Dodecane	8.30	carbamate	1.61	Diaziridine,3,3-dimethyl-	2.37
Cyclopropane, 2-bromo-1,1,3-trim...	4.38	Pilocarpine	4.44	-	0	Ethinamate	2.40	Pilocarpine	1.95	,4,7,10,13,16-Hexaoxacycloeicos	2.78
Tilidine-M	4.43	Dodecane	9.43	-	0	MECC	8.43	Ethirimol	5.84	2-Propenoic acid	2.67
5-Methyl-1-hexene	4.38	Naphthalene, decahydro-2,3-dimet	3.97	-	0	Pilocarpine	8.73	Fluorene	1.17	Oxalic acid, cyclohexyl pentyl e...	4.13
2-Methyl-1-pentene	4.23	Ethinamate	4.53	-	0	Ethirimol	7.83	Pyritinol	1.60	Chloroform	4.38
Oxalic acid, isobutyl nonyl ester	2.44	Cyclohexene,1-hexyl-	3.46	-	0	Ibuprofen-M (HO-) ME	5.69	Dodecane	7.35	Nonadecane	2.07

1-Octadecyne	0.00	MECC	7.03	-	0	Terbutaline -H2O 2AC	5.88	Pilocarpine	3.40	Bicyclo[3.1.0]hexane, 1,5-dimethyl-	3.69
Cyclohexene, 1-hexyl-	3.15	Paracetamol	5.17	-	0	-	0	1-Octadecyne	2.03	Camphor \$\$ Bicyclo[2.2.1]heptan	3.80
5-Undecyne	3.19	Ibuprofen-M (HO-) ME	3.14	-	0	-	0	MECC	7.23	Pilocarpine	3.31
Citronellyl propionate	3.90	2-Propenoic acid, 3-phenyl-	2.93	-	0	-	0	Paracetamol	4.29	2-Penten-4-yn-1-ol, 3-methyl-, (E)-	2.04
L-(-)-Menthol	3.15	Tioconazole	3.56	-	0	-	0	Naphthalene, decahydro-1,5-dimet	6.74	rac-2,4-Dimethyl-3-nitrobicyclo	2.35
Dodecane	5.77	-	0	-	0	-	0	Ethinamate	7.29	Ethinamate	1.80
3,4-Octadiene, 7-methyl-	2.61	-	0	-	0	-	0	Gabapentin -H2O ME	6.74	DOM	4.55
MECC	2.14	-	0	-	0	-	0	Ibuprofen-M (HO-) ME	1.92	Paracetamol	2.76
Pilocarpine	2.36	-	0	-	0	-	0	-	0	Tridecane	2.34
Gabapentin -H2O ME	4.65	-	0	-	0	-	0	-	0	Hexadecane	2.23

Gabapentin -H ₂ O ME	3. 39	-	0	-	0	-	0	-	0	2-Propenoyl chloride, 3-phenyl	2.9 9
Paracetamol	3. 53	-	0	-	0	-	0	-	0	Azinphos-methyl	3.6 9
Ethinamate	5. 47	-	0	-	0	-	0	-	0	urea, N'-[4-(2- formylhydrazinyl)..	17. 52

Carbohydrate (Polysaccharide) Content

Statistical analysis showed no significant differences in carbohydrate content among populations at the county level. However, habitat-specific variations within counties were significant at $p < 0.01$ (Table

3). The mean carbohydrate content was 366.93 mg glucose equivalent per gram (mg GE/g). The maximum polysaccharide content (577 mg GE/g) was found in the Saravan population, whereas the minimum (171.3 mg GE/g) was recorded in Nahoak (Table 4).

Table 3: Analysis of variance (ANOVA) of total phenolic, flavonoid, and carbohydrate contents in six populations of the medicinal plant *A. fasciculifolius*

Source of Variation	df	Phenolics	Flavonoids	Carbohydrates
Mean Squares				
County	2	97.45*	1.69**	2034.85 ns
Location×County	3	65.79**	1.21**	107474.47**
Error	12	4.46	0.009	824.40
CV (%)		6.52	6.40	7.82

*, **, ns, respectively in 5, and 1 level and none significant.

Table 4: Phytochemical composition of *A. fasciculifolius* gum resin from different habitats in Sistan and Baluchestan Province

No.	Habitat	Phenolics (mg GAE/g)	Flavonoids (mg QE/g)	Carbohydrates (mg GE/g)
1	Saravan	29.0 ± 3.32	1.0 ± 0.11	577.5 ± 30.45
2	Nahoak	28.1 ± 3.44	2.0 ± 0.33	171.7 ± 18.3
3	Birak	31.0 ± 4.22	0.0 ± 0.0	414.1 ± 25.68
4	Anjirak	30.2 ± 3.11	1.0 ± 0.15	346.7 ± 22.78
5	Poshtkuh	31.3 ± 3.85	1.0 ± 0.23	452.3 ± 28.98
6	Panjangasht	42.1 ± 4.46	1.0 ± 0.12	240.1 ± 19.11

Parameter optimization for silver nanoparticles synthesis

200 mL of Anzerot root and gum extract were combined with 100 mL of a 1 mM silver nitrate solution, then diluted with distilled water to a total volume of 500 mL. A color change from white to red or brown was subsequently observed, indicating successful synthesis of silver nanoparticles (SNPs). UV-Vis spectroscopy results showed that the SNPs exhibited the highest absorption within the wavelength range of 400-500 nm, a phenomenon associated with the surface plasmon resonance (SPR) of the nanoparticles.

AgNPs Characterization by TEM and XRD analysis

The results revealed diffraction peaks at 38°, 43°, 64°, and 77.30°, which correspond to the

crystallographic planes (111), (200), (220), and (311) of the face-centered cubic Ag nanocrystals. These findings are in line with previous studies.

The XRD analysis revealed the crystalline structure of *A. fasciculifolius* GS-AgNPs. The average crystal size of the silver nanoparticles produced during bioreduction was calculated using Scherer's equation. The values for gum and root extracts nanoparticles were measured as 23.29 nm and 15.28 nm, respectively. TEM examination was conducted in order to determine the morphological properties of the synthesized AgNPs. According to the TEM analysis, the synthesized AgNPs exhibited a spherical or pseudo-spherical shape (Figure 2). TEM analysis of the biosynthesized silver nanoparticles revealed that the nanoparticle sizes for Anzaroot root and gum nanoparticles range from 5-50 nm and 12-26 nm, respectively.

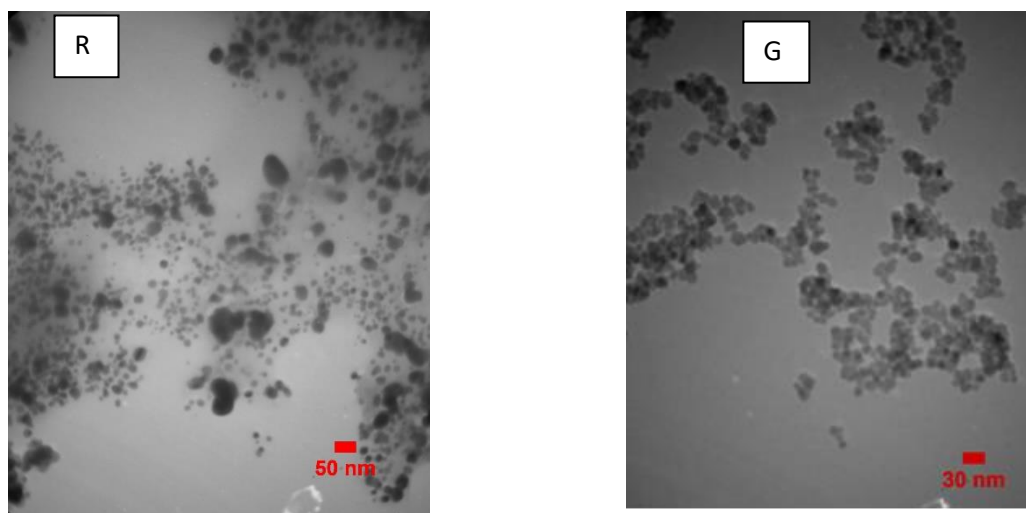


Figure 2: TEM analysis of biosynthesized silver nanoparticle from Anzaroot Root (R) and Gum (G) extracts

DPPH free radical scavenging (FRS) activity

Free radical scavenging (FRS) is of critical importance due to the deleterious effects of reactive oxygen species on biological systems. The 2,2-diphenyl-1-picrylhydrazyl (DPPH) radical, a stable lipophilic nitrogen-centered radical, serves as a widely employed model for evaluating the efficacy of antioxidant compounds. Among various analytical techniques, the DPPH assay offers a rapid and reliable method for screening the radical

scavenging potential of anticancer agents. In this study, we investigated the FRS capacity of *A. fasciculifolius* root and gum extracts, along with their corresponding biosynthesized nanoparticles, at concentrations of 100, 200, 300, 400, and 500 µg/mL. As illustrated in Figure 3, a dose-dependent enhancement in antioxidant activity was observed with increasing concentrations of both nanoparticles and crude extracts. Notably, the gum-derived compounds exhibited superior radical scavenging efficacy compared to their root-based counterparts. Quantitative analysis revealed that at 500 µg/mL, the FRS activity of gum nanoparticles (98.40%) significantly exceeded that of root nanoparticles (81.41%). Similarly, the gum extract (70.94%)

demonstrated higher antioxidant potency than the root extract (60.94%). These findings underscore the

enhanced bioactivity of gum-based formulations in neutralizing free radicals.

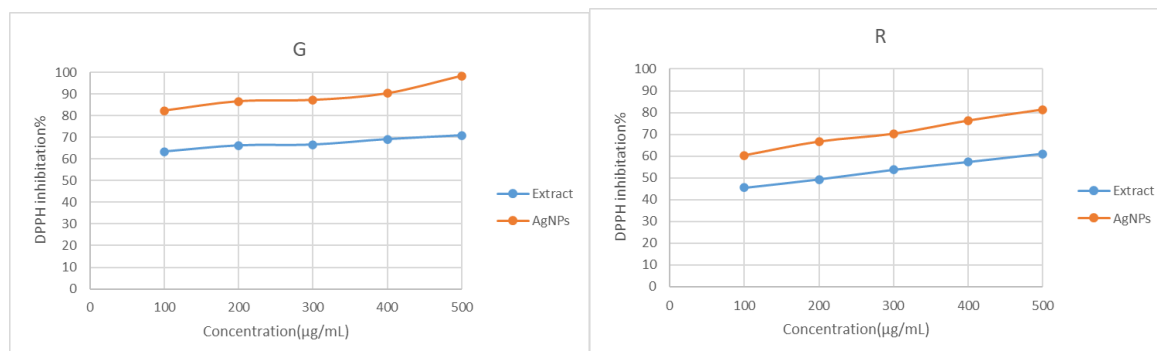


Figure 3: The DPPH FRS activity of the *A. fasciculifolius* root and gum extracts and its GS-AgNPs at different extracts concentrations

Antibacterial Activity Disc Diffusion Method

Table 5 displays the antimicrobial efficacy of Anzaroot (*A. fasciculifolius*) root and gum extracts along with their corresponding green-synthesized silver nanoparticles (GS-AgNPs) at a standardized concentration of 400 µg/mL against selected Gram-negative (*Escherichia coli* and *Pseudomonas aeruginosa*) and Gram-positive (*Bacillus cereus* and *Staphylococcus aureus*) bacterial pathogens. The disk diffusion assay results demonstrated that both crude extracts and biosynthesized nanoparticles

exhibited fundamental antibacterial properties against all tested microorganisms. However, a distinct antimicrobial pattern emerged: the GS-AgNPs displayed superior inhibitory effects against Gram-negative strains compared to Gram-positive organisms. Conversely, the phytochemical extracts of Anzaroot (both root and gum) manifested greater antibacterial potency against Gram-positive bacteria relative to their Gram-negative counterparts. Overall, the antibacterial activity of Anzaroot GS-AgNPs against both Gram-(negative and positive) bacterial strains was higher as compared to that of root and gum extract.

Table 5: The antibacterial activities of *A. fasciculifolius* Bioss root and gum extracts and its green synthesized silver nanoparticles against various bacterial strains

Bacteria	MIC (µg/mL)					MBC (µg/mL)				
	Root	R	Gum	G	AMP	Root	R	Gum	G	AMP
<i>E. coli</i>	100	100	200	50	100	200	50	200	25	100
<i>B. cereus</i>	200	50	200	25	50	200	50	200	25	100
<i>S. aureus</i>	200	3.12	400	3.12	200	400	3.12	400	6.25	200
<i>P. aeruginosa</i>	50	6.25	400	3.12	100	200	6.25	200	12.5	100

Root Extract (Root), RootNPs(R), Gum Extract (Gum), Gum NPs (G), Ampicillin (AMP).

Ingredients of Anzeroot root and gum extract

Discussion

Silver has been known as a 'dynamic' agent because of its exceptional potential for diverse biological applications. It can act as an anti-fungal, anti-bacterial, anti-viral, anti-inflammatory and wound-healing agent, even at low concentrations. Most importantly, it is a non-toxic inorganic antibacterial agent, showing anti-infectious activity against approximately 650 pathogenic microorganisms [27, 28]. The use of AgNPs in various commercial products is on the rise worldwide. Consequently, living organisms are being exposed to nanoparticles, either intentionally or unintentionally, an event which raises concerns about nanoparticle toxicity. Thus, it is essential to establish the proper application of nanoparticles for different biological purposes. Nanoparticle green synthesis has already shown potential as a safe and environmentally-friendly method. This method allows for the cost-effective mass production of nanoparticles [28].

UV-visible spectrophotometric analysis verified the successful biosynthesis of silver nanoparticles (AgNPs) through detection of a characteristic absorption peak corresponding to surface plasmon resonance (SPR). This optical phenomenon results from coherent electron charge oscillations at the nanoparticle surface when interacting with incident electromagnetic radiation, consistent with established theoretical frameworks. The extinction coefficient of the SPR peak serves as a quantitative indicator of nanoparticle production efficiency. Furthermore, the spectral position (λ_{max}) and full-width at half-maximum (FWHM) of the SPR band correlate strongly with critical nanoparticle characteristics including mean particle diameter, morphological features, and degree of aggregation [29]. The presence of a peak at 445 nm in the UV-vis absorption spectrum of our GS-AgNPs indicates the occurrence of SPR absorption, hence confirming a successful AgNPs synthesis. Moreover, mixing Anzaroot extract with silver salt solution resulted in a solution color change from white to reddish brown which further support the effectiveness of our SNPs synthesis. The occurrence of a strong band in UV-vis absorption spectrum of the GS-AgNPs can be attributed to the plasmon resonance, which involves electrons oscillations on the surface of the silver nanoparticles [30].

Astragalus plants have been used in green synthesis of silver nanoparticles in several studies. The antimicrobial effects of these green synthesized

nanoparticles have been extensively studied, as well. Assessment of the antimicrobial activity of *Astragalus atropilosulus* subsp. *Abyssinicus* leaf extract against various pathogenic bacteria using agar well diffusion method demonstrated the inhibition zone with sizes ranging from 9.33 mm to 35.0 mm. [31]. In another study on biosynthesis of antibacterial AgNPs using *Astragalus* versus *Olivier* various factors including temperature, pH level and the concentration of tragacanth as the extraction medium, were employed. The findings demonstrated the successful green synthesis of AgNPs with a spherical morphology and an average diameter of approximately 40 nm. Furthermore, the results of antibacterial assays validated the significant antibacterial activity of the biosynthesized AgNPs [32]. The synthesis of biologically active AgNPs using *Astragalus sarcocolla* red and yellow gums at different concentrations demonstrated effective antimicrobial properties against various gram-positive and gram-negative bacterial strains [33].

The biosynthesized Anzaroot silver nanoparticles (AgNPs) exhibited broad-spectrum antimicrobial efficacy, demonstrating MIC/MBC values ranging from 3.12 to 400 $\mu\text{g/mL}$ across all tested microbial strains, with no statistically significant differences observed between root and gum extracts ($p > 0.05$) or their respective nanoparticle formulations. However, gum-derived nanoparticles (G-NPs) showed enhanced antibacterial performance, likely attributable to their reduced particle size, as antimicrobial activity was determined to be dependent on synthesis methodology, nanoscale dimensions, and concentration gradients. The nanoparticles displayed strongest inhibition against *Pseudomonas aeruginosa* and weakest against *Staphylococcus aureus*, with generally greater efficacy against Gram-positive organisms (except *Streptococcus pyogenes*) compared to Gram-negative strains. This differential susceptibility stems from fundamental structural differences in bacterial cell envelopes: Gram-negative bacteria possess a thin peptidoglycan layer (7-8 nm) surrounded by an asymmetric outer membrane containing lipopolysaccharides, while Gram-positive species feature a thick, multilayered peptidoglycan matrix (30-100 nm) without an outer membrane. The Gram-positive peptidoglycan architecture, composed of N-acetylglucosamine-N-acetylmuramic acid polymers with 6-7 acyl chains, core oligosaccharides, and O-antigen polysaccharides, forms a selectively permeable

barrier that excludes hydrophilic molecules >700 Da while providing protection against osmotic stress. These structural characteristics collectively contribute to the observed variation in antimicrobial susceptibility patterns between bacterial classes [34].

Based on our findings, it was observed that both Anzaroot root and gum AgNPs have a higher antioxidant activity compared to their respective extracts. This aligns with the research conducted by Sharifi-Rad et al, who also reported that *A. tribuloides* GS-AgNPs exhibited higher antioxidant activity (64%) compared to *A. tribuloides* root extract (47%) [35]. Moreover, it has shown that AgNPs synthesized using *Petroselinum crispum* seed extract at the concentrations of 125 and 250 µg/mL, can inhibit DPPH radicals by 93% and 96%, respectively [36]. In another [37], The investigation revealed that AgNPs, which were synthesized using *Sophora pachycarpa* extract (SPE-AgNPs), displayed approximately 30% inhibition of DPPH radicals at a concentration of 0.8 µg/mL. The antioxidant activity of the *S. pachycarpa* extract was comparatively lower than that of SPE-AgNPs. For instance, the *S. pachycarpa* extract demonstrated around 60% inhibition of DPPH radicals at a concentration of 5 mg/mL [37]. Spectrophotometric analysis revealed a concentration-dependent enhancement in DPPH radical scavenging capacity, with inhibition percentages escalating from 14% to 98% as the concentration of *Astragalus sarcocolla*-derived gum extract nanoparticles (ASG-AgNPs) increased from 100 to 800 µg/mL. This pronounced dose-response relationship demonstrates remarkable free radical neutralization potential. Phytogetic antioxidants of this nature represent viable substitutes for conventional synthetic preservatives, particularly butylated hydroxyanisole (BHA) and butylated hydroxytoluene (BHT), which are extensively employed as oxidative stabilizers in food processing applications. This is important due to the potential mutagenic effects associated with these synthetic options. Natural antioxidants, such as *A. fasciculifolius* B. in the form of root and gum extract or GS-AgNPs, can help protect the body against oxidative damage. Ultimately, this protective strategy may aid in preventing degenerative conditions related to compromised health [38].

Our findings align with prior investigations [29, 39] demonstrating that phytogetic synthesis of silver nanoparticles employing *E. japonica* foliar extract

was visually evidenced by a chromatic transition in the silver nitrate solution from transparent to amber-brown. Spectrophotometric analysis further corroborated nanoparticle formation through the manifestation of a well-defined surface plasmon resonance (SPR) peak centered at approximately 435 nm, characteristic of metallic silver nanostructures [29, 39]. Complementary research by Rehab utilizing *Psidium guajava* leaf extract for nanofabrication yielded congruent results with established literature. X-ray diffraction analysis revealed four characteristic Bragg reflections at 2θ angles of 38°, 43°, 64°, and 76°, indexing to the 111, 200, 220, and 311 crystallographic planes of face-centered cubic silver, respectively. This diffraction pattern exhibits remarkable consistency with XRD profiles documented in studies employing *Astragalus membranaceus* root extract for nanoparticle biosynthesis [40].

The biosynthesis of silver nanoparticles using *A. tribuloides* root extract resulted in AgNPs with a spherical morphology, crystalline structure, and an average size of 34.2 nm. Antibacterial tests showed that the biosynthesized AgNPs exhibit significantly greater bactericidal activity against both Gram-positive and Gram-negative bacteria compared to the *A. tribuloides* root extract [35]. Several studies have explored the phytochemical content of various species within the *Astragalus* genus. Key metabolites identified in these species include triterpenoid saponins, flavonoids, and polysaccharides. These compounds exhibit significant medicinal properties, providing protection against serious diseases such as cancer, diabetes, immunodeficiency, liver damage, cardiovascular disorders, and inflammatory conditions. Therefore, it is essential to investigate the phytochemical and bioactive properties of these plants. The findings of this study confirm the presence of phytochemical compounds, including flavonoids, phenols, and polysaccharides, in both Anzaroot root and gum extracts. Using gas chromatography-mass spectrometry (GC-MS) method, it has been investigated [41] the volatile compounds of six *Astragalus* species. A total of 97 metabolites were identified. Sylvestrene was the most dominant component in *A. sieversianu*, *A. mucidus* and *A. macronyx* species, with *A. sieversianu* strain showing the highest content (64.64%). Nevertheless, (E)-2-hexenal was the major component in *A. chiwensis* (10.1%) and *A. lehmannianus* (9.97%) species. It has been analyzed

the composition of *Astragalus chrysostachys* Boiss root essential oil using GC-MS method. A total of 8 compounds including Linalool (2.4%), m-Tolualdehyde (29.7%), Undecane (0.4%), Hexahydrofarnesyl acetone (3.7%), and acetophenone (16.2%), Carotol (1.5%), Croweacin (12.3%) and Dodecene (9.9%) were detected.

Halogenated cyclohexanes, including 1-bromocyclohexane, show antimicrobial potential, particularly against bacterial and fungal pathogens, due to their bioactive halogen substituents. It is also used as a pharmaceutical intermediate in medicinal chemistry research [42]. While direct evidence is limited, structurally related dodecyl-containing compounds (e.g., dodecylglycerol) exhibit antibacterial properties, suggesting potential applications in combating microbial infections. Its synthesis methods may support the development of bioactive molecules [43]. Primarily used in pharmaceutical research as a synthetic intermediate, though specific therapeutic applications remain unclear [44]. No direct evidence links these compounds (3,4-Heptadiene and 3-Octyne) to human disease treatment in the provided data. They are typically employed in organic synthesis, which may indirectly contribute to drug discovery.

In the present study, we investigated the phytochemical composition of the gum and root extract of *A. fasciculifolius* Boiss species, for the first time. The highest amounts of hexadecane, tetradecane, and octadecane content were measured as 4.00%, 21.78%, and 7.81%, respectively. It was known that the gum extract contains a greater variety of compounds as compared to the root extract. *A. fasciculifolius* Boiss is the native plant of Sistan and Baluchestan province, Iran. It has a long history of traditional use in treating a wide range of diseases, such as cough, toothache, stomach ache, chest infection, heart disease, and cancer. It is believed that this plant can strengthen tooth roots, show considerable nutritional effects, and support kidney health. Though other studies have investigated the antioxidant and antibacterial properties of other *Astragalus* species there is a lack of scientific research on antioxidant and antibacterial profile of *A. fasciculifolius* Boiss species [45]. For example, a study conducted on the root extract of *Astragalus chrysostachys* Boiss, which are native to East Azarbaijan, Iran, showed that the ethyl acetate root extracts exhibit a significant antioxidant activity in the DPPH scavenging assay, with an IC₅₀ value of

14.6 µg/mL. The extracts revealed a mild antibacterial activity against Gram-positive bacteria, as well [46]. In another study, the extracts of different plant sections of *Astragalus adscondens* Boiss & Haussk species (also known as Persian Manna) demonstrated significant antioxidant activity. This indicates that this plant has the potential to be utilized as a natural source of antioxidants [45]. Although limited research has been conducted on the antioxidant and antibacterial properties of *A. fasciculifolius* Boiss, other *Astragalus* species have demonstrated promising results. Thus, further investigation is required in order to verify the antioxidant and antibacterial properties of *A. fasciculifolius* Boiss as well as its potential applications in phytotherapeutic practice [45, 46].

The antibacterial properties of AgNPs are primarily influenced by several factors such as the size and shape of nanoparticle and the pH and ionic strength of the synthetic environment, as well as the type of coating. Despite extensive research, the exact mechanism responsible for the antibacterial activity of AgNPs remains unclear. However, it is believed that they can exert their effects through three different mechanisms [47]. In the first one, it is assumed that nanoparticles exert their effects on the cell membrane surface. They can penetrate the bacterial outer membrane and subsequently accumulate within the inner cell membrane. Consequently, they enhance cell membrane permeability, resulting in the leakage of cellular contents, leading to bacterial cell death. Moreover, they can bind sulfur-containing proteins in the bacterial cell wall, causing structural damage and cell wall rupture. According to the second mechanism, nanoparticles not only possess the ability to traverse the cell membrane and modify its structure and permeability, but they can also penetrate the cell and interact with sulfur or phosphorous components of DNA and proteins. This interaction induces some alterations in the structure and function of these cell components. Similarly, nanoparticles may disrupt intracellular processes and impede ATP release through interaction with thiol groups in respiratory enzymes. These enzymes play a critical role in preventing oxidative stress through neutralizing reactive oxygen species and free radicals. The third proposed mechanism, which can occur in conjunction with the other two mechanisms, involves the release of silver ions by nanoparticles. These ions, owing to their size and charge, can

interact with cellular components and disrupt metabolic pathways, cell membranes, and even genetic material.

Phytochemical characterization of *Astragalus compactus* Lam. revealed differential distribution of bioactive constituents across its aerial and subterranean organs [48]. GC-MS analysis identified 19 distinct phytochemicals, with quantitative and qualitative variations observed among foliar, radicular, and gummiferous tissues. Notably, the root extract contained a unique chlorinated volatile organic compound among congeneric species, while the gum extract demonstrated exceptional purity with complete absence of toxic chlorinated derivatives. Parallel investigation of *Astragalus calliphysa* Bge. gum extract via ethanol extraction yielded 18 characterized compounds representing 99.6% of the total phytochemical profile. The major constituents comprised: n-hexadecane (19.29%), n-pentadecane (18.78%), n-tetradecane (15.36%), n-heptadecane (10.38%), polgone (9.25%), and n-octadecane (8.04%), demonstrating a predominance of aliphatic hydrocarbons in this medicinal exudate [49].

The retention index (RI) of ethylbenzene varies depending on gas chromatography (GC) column type and experimental conditions. For a HP-1 capillary column (30 m × 0.25 mm × 0.25 µm), ethylbenzene has an RI of 848.1 under helium carrier gas with a temperature program starting at 60°C. On a DB-5 capillary column (30 m × 0.32 mm × 0.25 µm), the RI increases to 864.1 under similar conditions [50, 51]. These differences arise from variations in stationary phase chemistry and temperature gradients. The RI is calculated using hydrocarbon references with the formula: $RI = 100n + 100(tx - tn)(tn + 1 - tn)$, where tx is the compound's retention time and tn , $n+1$ are reference hydrocarbon carbon numbers [51]. The retention index (RI) of 1,3-dimethylbenzene (m-xylene) varies based on chromatographic conditions. On a DB-5 capillary column (60 m × 0.32 mm × 1.0 µm), it has an RI of 867 under helium carrier gas with a temperature program starting at 40°C. For HP-5 columns, values range from 869 (30 m × 0.25 mm × 0.33 µm, 5°C/min) to 882.7–888.1 (60 m × 0.25 mm × 0.25 µm, unspecified temperature gradient). These differences highlight how column dimensions, stationary phase chemistry, and heating rates influence retention behavior. For example, it has been reported RIs of 882.7 and 888.1 for 1,3-

dimethylbenzene using two HP-5 columns with identical dimensions but different experimental parameters. Such variability underscores the need to reference specific methodologies when comparing retention indices [52]. The retention index of bromocyclohexane (1-bromocyclohexane) varies with chromatographic conditions. Under standard non-polar conditions, its Kovats retention index (RI) is 975, while in polar conditions, the RI rises to 1324. These differences reflect variations in stationary phase chemistry and separation mechanisms. The Kovats index, which is calculated using n-alkane references, provides a system-independent measure of retention behavior. For bromocyclohexane, structural features such as the bromine substituent and cyclohexane ring affect its interaction with the column phase, resulting in distinct RI values for polar versus non-polar setups. The NIST WebBook cites studies that utilize retention indices for structural identification but does not provide specific values for this compound [53, 54].

Conclusions

This study developed an eco-friendly method for synthesizing silver nanoparticles (AgNPs) using *A. fasciculifolius* extracts, serving as both reducing and capping agents. The spherical, crystalline AgNPs (5–50 nm) showed strong LSPR absorption at 445 nm. Geographic variations affected plant phytochemistry (phenolics: 28.1–42.6 mg GAE/g; flavonoids: 0–2 mg QE/g). The biosynthesized AgNPs exhibited exceptional antioxidant (98.4% scavenging) and antibacterial activity (MIC 3.12–50 µg/mL), outperforming crude extracts. These results demonstrate the method's efficiency and the nanoparticles' significant potential for biomedical applications, particularly in novel drug therapies.

Abbreviation

DPPH: 2,2-diphenyl-1-picrylhydrazyl radical; FRS: free radical scavenging; GS-AgNPs: green synthesized AgNPs; MBC: Minimum Bactericidal Concentration; MIC: Minimum Inhibitory Concentration; PXRD: power X-ray diffraction; TEM: transmission electron microscopy

Conflict of Interests

All authors declare no conflict of interest.

Ethics approval and consent to participate

No human or animals were used in the present research.

Ethical issues

Ethical issues (including plagiarism, data fabrication, double publication) have been completely observed by the authors. The authors have adhered to ethical standards, including avoiding plagiarism, data fabrication, and double publication.

Consent for publication

All authors read and approved the final manuscript for publication.

Availability of data and material

All the data are embedded in the manuscript.

Authors' contributions

Conceptualization: B. F-N., F.N.; Data curation: F. N.; Formal analysis: H. Gh.; Investigation: R. Sh.; Methodology: B. F-N., F.N.; Project administration: B. F-N.; Resources: All authors.; Supervision: B. F., N. M.; Validation: B. F.; Visualization: R. Sh.; Writing—original draft: F. N., B. Z-N.; Writing—reviewing & editing: All authors.

Informed Consent

The authors declare not used any patients in this research.

Acknowledgement

This article was achieved based on the material and equipment of Agricultural Biotechnology Research Institute, University of Zabol, that the authors thanks it

Funding/Support

The support fund of the Iranian National Science Foundation (INFS) has been placed with the project code 4004761.

References

1. Shahdadi F, Khorasani S, Salehi-Sardoei A, Fallahnajmabadi F, Fazeli-Nasab B, Sayyed RZ. GC-MS profiling of *Pistachio vera* L., and effect of antioxidant and antimicrobial compounds of it's essential oil compared to chemical counterparts. *Sci*

- Rep. 2023;13(1):21694. doi:<https://doi.org/10.1038/s41598-023-48844-5>.
2. Javadian E, Biabangard A, Ghafari M, Saeedi S, Fazeli-Nasab B. Green Synthesis of Silver Nanoparticles and Antibacterial Properties of Extracts of *Capparis spinosa* Leaves. *Int J Med Plants By-Prod.* 2024;13(2):329-43. doi:<https://doi.org/10.22034/jmpb.2023.361363.1528>.
3. Alavi M, Hamblin MR, Aghaie E, Mousavi SAR, Hajimolaali M. Antibacterial and antioxidant activity of catechin, gallic acid, and epigallocatechin-3-gallate: focus on nanoformulations. *Cell Mol Biomed Rep.* 2023;3(2):62-72. doi:<https://doi.org/10.55705/cmbr.2022.353962.1052>.
4. Saravani S, Ghaffari M, Aali H. Hydroalcoholic extract of *Psidium guajava* plant and bone marrow cells: examination and analysis of effects. *Cell Mol Biomed Rep.* 2024;4(3):177-1888. doi:<https://doi.org/10.55705/cmbr.2024.428153.1213>.
5. Saravani K, Akbari ME, Akbari MM, Fazeli-Nasab B. The Protective Effect of Hydro-alcoholic Extracts of Cactus Fruit (*Opuntia dillenii* (Ker Gawl.) Haw.) and Star Fruit (*Averrhoa carambola* L.) on Histological Changes Induced by Cadmium Chloride in Lungs of Male Wistar Rats. *Int J Med Plants By-Prod.* 2023;12(3):267-74. doi:<https://doi.org/10.22092/jmpb.2022.356472.1421>.
6. Daneshmand S, Niazi M, Fazeli-Nasab B, Asili J, Golmohammadzadeh S, Sayyed RZ. Solid Lipid Nanoparticles of *Platycladus orientalis* L. possessing 5-alpha Reductase Inhibiting Activity for Treating Hair Loss and Hirsutism. *Int J Med Plants By-Prod.* 2023;13(1):233-46. doi:<https://doi.org/10.22034/jmpb.2023.364389.1634>.
7. Taha ZK, Hawar SN, Sulaiman GM. Extracellular biosynthesis of silver nanoparticles from *Penicillium italicum* and its antioxidant, antimicrobial and cytotoxicity activities. *Biotechnol Letters.* 2019;41:899-914. doi:<https://doi.org/10.1007/s10529-019-02699-x>.
8. Karnani RL, Chowdhary A. Biosynthesis of silver nanoparticle by eco-friendly method. *Int J Nanosci.* 2013;1(1):25-31.
9. Chaudhary LB, Rana TS, Anand KK. Current status of the systematics of *Astragalus* L.(Fabaceae) with special reference to the Himalayan species in India. *Taiwania.* 2008;53(4):338-55.

10. Zarre S, Azani N. Perspectives in taxonomy and phylogeny of the genus *Astragalus* (Fabaceae): a review. *PBioSci*. 2013;3(1):1-6.
11. Li X, Qu L, Dong Y, Han L, Liu E, Fang S, et al. A Review of Recent Research Progress on the *Astragalus* Genus. *Molecules*. 2014;19(11):18850-80. doi:<https://doi.org/10.3390/molecules191118850>. [PubMed:doi:10.3390/molecules191118850].
12. Huang C, Xu D, Xia Q, Wang P, Rong C, Su Y. Reversal of P-glycoprotein-mediated multidrug resistance of human hepatic cancer cells by Astragaloside II. *J Pharm Pharmacol*. 2012;64(12):1741-50. doi:<https://doi.org/10.1111/j.2042-7158.2012.01549.x>.
13. Lu J, Chen X, Zhang Y, Xu J, Zhang L, Li Z, et al. *Astragalus* polysaccharide induces anti-inflammatory effects dependent on AMPK activity in palmitate-treated RAW264. 7 cells. *Int J Mol Med*. 2013;31(6):1463-70. doi:<https://doi.org/10.3892/ijmm.2013.1335>.
14. Benchadi W, Haba H, Lavaud C, Harakat D, Benkhaled M. Secondary metabolites of *Astragalus cruciatus* Link. and their chemotaxonomic significance. *Rec Nat Prod*. 2013;7(2):105-13.
15. Linnek J, Mitaine-Offer AC, Miyamoto T, Tanaka C, Paululat T, Avunduk S, et al. Cycloartane glycosides from three species of *Astragalus* (Fabaceae). *Helvetica Chimica Acta*. 2011;94(2):230-7. doi:<https://doi.org/10.1002/hlca.201000157>.
16. El-Rafie M, El-Naggar M, Ramadan M, Fouda MM, Al-Deyab SS, Hebeish A. Environmental synthesis of silver nanoparticles using hydroxypropyl starch and their characterization. *Carbohydrate Polymers*. 2011;86(2):630-5.
17. Gao Y, Chen Y, Ji X, He X, Yin Q, Zhang Z, et al. Controlled intracellular release of doxorubicin in multidrug-resistant cancer cells by tuning the shell-pore sizes of mesoporous silica nanoparticles. *ACS nano*. 2011;5(12):9788-98.
18. Das D, Nath BC, Phukon P, Dolui SK. Synthesis and evaluation of antioxidant and antibacterial behavior of CuO nanoparticles. *Colloids and Surfaces B: Biointerfaces*. 2013;101:430-3.
19. Qu M, Zhang X, Liu G, Huang Y, Jia L, Liang W, et al. An eight-year study of *Shigella* species in Beijing, China: serodiversity, virulence genes, and antimicrobial resistance. *J Infect Dev Ctries*. 2014;8(07):904-8. doi:10.3855/jidc.3692.
20. Chang C-C, Yang M-H, Wen H-M, Chern J-C. Estimation of total flavonoid content in propolis by two complementary colorimetric methods. *Journal of food and drug analysis*. 2002;10(3):178-82.
21. McDonald S, Prenzler PD, Antolovich M, Robards K. Phenolic content and antioxidant activity of olive extracts. *Food Chemistry*. 2001;73(1):73-84. doi:[https://doi.org/10.1016/S0308-8146\(00\)00288-0](https://doi.org/10.1016/S0308-8146(00)00288-0).
22. Rover MR, Johnston PA, Lamsal BP, Brown RC. Total water-soluble sugars quantification in bio-oil using the phenol-sulfuric acid assay. *Journal of Analytical and Applied Pyrolysis*. 2013;104:194-201. doi:<https://doi.org/10.1016/j.jaap.2013.08.004>.
23. Yue F, Zhang J, Xu J, Niu T, Lü X, Liu M. Effects of monosaccharide composition on quantitative analysis of total sugar content by phenol-sulfuric acid method. *Frontiers in nutrition*. 2022;9:963318. doi:<https://doi.org/10.3389/fnut.2022.963318>.
24. Shamspur T, Sheikhshoae I, Afzali D, Mostafavi A, Mirtadzadini S. Chemical Compositions of *Salix aegyptiaca* L. Obtained by Simultaneous Hydrodistillation and Extraction. *J Essent Oil-Bear Plants*. 2011;14(5):543-8. doi:<https://doi.org/10.1080/0972060X.2011.10643971>.
25. Zarnowski R, Suzuki Y. Expedient Soxhlet extraction of resorcinolic lipids from wheat grains. *J Food Compos Anal*. 2004;17(5):649-63. doi:<https://doi.org/10.1016/j.jfca.2003.09.007>.
26. Mamidipally PK, Liu SX. First approach on rice bran oil extraction using limonene. *Eur J Lipid Sci Technol*. 2004;106(2):122-5. doi:<https://doi.org/10.1002/ejlt.200300891>.
27. Morton JF. Fruits of warm climates. JF Morton; 1987. p. 517 Pages.
28. Verma K, Shrivastava D, Kumar G. Antioxidant activity and DNA damage inhibition in vitro by a methanolic extract of *Carissa carandas* (Apocynaceae) leaves. *Journal of Taibah University for science*. 2015;9(1):34-40.
29. Dastafkan K, Khajeh M, Bohlooli M, Ghaffari-Moghaddam M, Sheibani N. Mechanism and behavior of silver nanoparticles in aqueous medium as adsorbent. *Talanta*. 2015;144:1377-86.
30. Amendola V, Bakr OM, Stellacci F. A study of the surface plasmon resonance of silver nanoparticles by the discrete dipole approximation method: effect of shape,

- size, structure, and assembly. *Plasmonics*. 2010;5:85-97.
31. Alrumman SA, Moustafa MF, Alamri SA. Anti-bacterial and anti-fungal investigation of *Astragalus atropilosulus* subsp. *abyssinicus*. *Afr J Microbiol Res*. 2012;6(34):6365-9. doi:<https://doi.org/10.5897/AJMR12.778>.
 32. Askari Z, Vahabi MR, Allafchian A, Mousavi SA, Jalali SAH. Biosynthesis of antibacterial silver nanoparticles using *Astragalus verus* Olivier. *Micro & Nano Letters*. 2020;15(2):66-71. doi:<https://doi.org/10.1049/mnl.2019.0306>.
 33. Abd El Aty AA, Alshammari SO, Alharbi RM, Soliman AA. *Astragalus sarcocolla* Gum-mediated a Novel Green-synthesis of Biologically Active Silver-Nanoparticles with Effective Anticancer and Antimicrobial activities. *Jordan J Biol Sci*. 2023;16(1):41-53. doi:<https://doi.org/10.54319/jjbs/160107>.
 34. Nikaido H. Molecular basis of bacterial outer membrane permeability revisited. *Microbiol Mol Biol*. 2003;67(4):593-656. doi:<https://doi.org/10.1128/mmbr.67.4.593-656.2003>.
 35. Sharifi-Rad M, Pohl P, Epifano F, Álvarez-Suarez JM. Green synthesis of silver nanoparticles using *Astragalus tribuloides* delile. root extract: Characterization, antioxidant, antibacterial, and anti-inflammatory activities. *Nanomaterials*. 2020;10(12):2383. doi:<https://doi.org/10.3390/nano10122383>.
 36. Zare-Bidaki M, Aramjoo H, Mizwari ZM, Mohammadparast-Tabas P, Javanshir R, Mortazavi-Derazkola S. Cytotoxicity, antifungal, antioxidant, antibacterial and photodegradation potential of silver nanoparticles mediated via *Medicago sativa* extract. *Arab J Chem*. 2022;15(6):103842. doi:<https://doi.org/10.1016/j.arabjc.2022.103842>.
 37. Kiani Z, Aramjoo H, Chamani E, Siami-Aliabad M, Mortazavi-Derazkola S. In vitro cytotoxicity against K562 tumor cell line, antibacterial, antioxidant, antifungal and catalytic activities of biosynthesized silver nanoparticles using *Sophora pachycarpa* extract. *Arab J Chem*. 2022;15(3):103677. doi:<https://doi.org/10.1016/j.arabjc.2021.103677>.
 38. Lim D-H, Choi D, Choi O-Y, Cho K-A, Kim R, Choi H-S, et al. Effect of *Astragalus sinicus* L. seed extract on antioxidant activity. *J Ind Eng Chem*. 2011;17(3):510-6. doi:<https://doi.org/10.1016/j.jiec.2011.02.040>.
 39. Mikhailova EO. Silver nanoparticles: Mechanism of action and probable bio-application. *Journal of functional biomaterials*. 2020;11(4):84.
 40. Ma Y, Liu C, Qu D, Chen Y, Huang M, Liu Y. Antibacterial evaluation of silver nanoparticles synthesized by polysaccharides from *Astragalus membranaceus* roots. *Biomedicine & Pharmacotherapy*. 2017;89:351-7.
 41. Gad HA, Mamadaliyeva NZ, Böhmendorfer S, Rosenau T, Zengin G, Mamadaliyeva RZ, et al. GC-MS based identification of the volatile components of six *Astragalus* species from Uzbekistan and their biological activity. *Plants*. 2021;10(1):124. doi:<https://doi.org/10.3390/plants10010124>.
 42. Islam M, Hossain A, Yamari I, Abchir O, Chtita S, Ali F, et al. Synthesis, Antimicrobial, Molecular Docking Against Bacterial and Fungal Proteins and In Silico Studies of Glucopyranoside Derivatives as Potent Antimicrobial Agents. *Chem Biodivers*. 2024;21(9):e202400932. doi:10.1002/cbdv.202400932. [PubMed:38949892].
 43. Huang G, Cierpicki T, Grembecka J. Thioamides in medicinal chemistry and as small molecule therapeutic agents. *Eur J Med Chem*. 2024;277:116732. doi:10.1016/j.ejmech.2024.116732. [PubMed:39106658].
 44. Yan X, Liu X, Zhao C, Chen GQ. Applications of synthetic biology in medical and pharmaceutical fields. *Signal Transduct Target Ther*. 2023;8(1):199. doi:10.1038/s41392-023-01440-5. [PubMed:37169742].
 45. Hassanpouraghdam MB, Ghorbani H, Esmaeilpour M, Alford MH, Strzemski M, Dresler S. Diversity and Distribution Patterns of Endemic Medicinal and Aromatic Plants of Iran: Implications for Conservation and Habitat Management. *Int J Environ Res Public Health*. 2022;19(3):1552. doi:<https://doi.org/10.3390/ijerph19031552>. [PubMed:doi:10.3390/ijerph19031552].
 46. Ghasemian-Yadegari J, Hamedeyazdan S, Nazemiyeh H, Fathiazad F. Evaluation of Phytochemical, Antioxidant and Antibacterial Activity on *Astragalus Chrysostachys* Boiss. *Roots*. *Iran J Pharm Res*. 2019;18(4):1902-11. doi:<https://doi.org/10.22037/2Fijpr.2019.1100855>. [PubMed:32184856].
 47. Bruna T, Maldonado-Bravo F, Jara P, Caro N. Silver nanoparticles and their antibacterial applications. *Int J Mol Sci*.

- 2021;22(13):7202.
doi:<https://doi.org/10.3390/ijms22137202>.
48. Movafeghi A, Djozan D, Razeghi J, Baheri T. Identification of volatile organic compounds in leaves, roots and gum of *Astragalus compactus* Lam. using solid phase microextraction followed by GC-MS analysis. *Natural Product Research*. 2010;24(8):703-9.
doi:<https://doi.org/10.1080/14786410802361446>.
 49. Shamspur T, Motasadizadeh H. Extraction chemical composition in the gum tragacanth of *Astragalus calliphysa* bge by soxhelt and identification composition using GC/MS. *J Sep Sci*. 2015;7(1):55-62.
doi:<https://doi.org/10.22103/jsse.2015.871>
 50. Wang Y, Liu J, Li N, Shi G, Jiang G, Ma W. Preliminary study of the retention behavior for different compounds using cryogenic chromatography at different initial temperatures. *Microchemical Journal*. 2005;81(2):184-90.
doi:<https://doi.org/10.1016/j.microc.2005.02.003>.
 51. Wang J-R, Wu X-Y, Cui C-B, Bi J-F. Effect of osmotic dehydration combined with vacuum freeze-drying treatment on characteristic aroma components of peach slices. *Food Chemistry: X*. 2024;22:101337.
doi:<https://doi.org/10.1016/j.fochx.2024.101337>.
 52. Koutek B, Fulem M, Mahnel Ts, Šimáček P, Růžicka Kt. Extracting Vapor Pressure Data from Gas–Liquid Chromatography Retention Times. Part 2: Analysis of Double Reference Approach. *Journal of Chemical & Engineering Data*. 2018;63(12):4649-61.
doi:<https://doi.org/10.1021/ACS.JCED.8B00699>.
 53. Khrisanfov MD, Matyushin DD, Samokhin AS. A general procedure for finding potentially erroneous entries in the database of retention indices. *Anal Chim Acta*. 2024;1297:342375.
doi:10.1016/j.aca.2024.342375.
[PubMed:38438243].
 54. Yang X, Li C, Qi M, Qu L. Graphene-ZIF8 composite material as stationary phase for high-resolution gas chromatographic separations of aliphatic and aromatic isomers. *J Chromatogr A*. 2016;1460:173-80. doi:10.1016/j.chroma.2016.07.029.
[PubMed:27423773].